Computational Physics

PHYS-3600 (Fall 2022)

Orbital Resonances: Kirkwood gaps

(Dated: Thursday December 1st, 2022)

CONTENTS

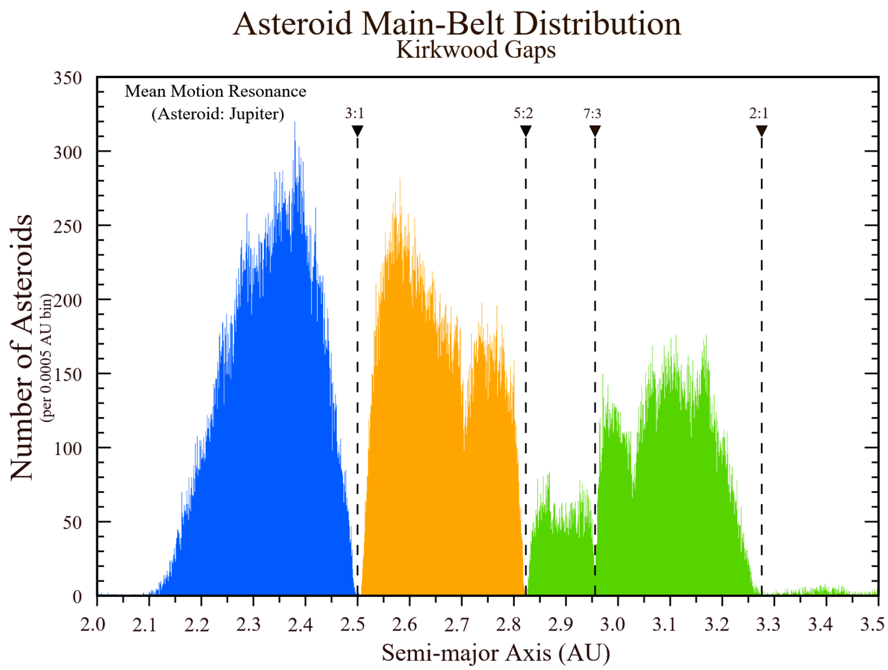

FIG. 1. Histogram of the known bodies in the asteroid belt, binned according to the length of their semi-major axis. Clearly gaps are visible at periods corresponding to 3:1, 5:2, 7:3 and 2:1 resonances with Jupiter's orbit. Source: [1].

I. INTRODUCTION

This project aims to examine the stability of orbiting bodies in the solar system to perturbations. In particular it will focus on the stability of orbits in the restricted three-body problem, where two heavy objects (in our case the Sun and Jupiter) affect a smaller body (an asteroid).

The most dramatic and best studied example of this physics in the solar system appears in the asteroid belt. Recall that the asteroid belt consists of a large number small bodies distributed between the orbits of Mars and Jupiter (roughly in the range of 2 AU to 3.5 AU from the Sun). While the distribution of these bodies appears to be mostly uniform, a peculiar structure appears if the known asteroids are categorized by the length of the semi-major axis of their orbit. While there are asteroids for most values of the semi-major axis (in their prescribed domain), there are a handful of of values that show an *absence* of asteroids. These "gaps" in the distribution appear at particular values of the semi-major axis: those whose periods are simple fractions of Jupiter's period. These are the so-called *Kirkwood gaps* [2]. Most prominent are the depletion at ratios of 3:1, 5:2, 7:3 and 2:1 as illustrated in Fig. 1. Orbits with these kinds of simple rational relationships are said to be in *resonance* with Jupiter and tend to feel the effect of its gravity more strongly than more generic, non-resonant orbits.

In this report we will explore the origin of these gaps using a direct numerical simulations of the orbits of small bodies under the combined effects of Jupiter and the Sun. We will first show that orbits that are in resonance with Jupiter do in fact fell Jupiter's gravity more significantly, causing a depletion of asteroids near these values of semi-major axis. While qualitatively correct, this observation alone does not reproduce the detailed structure of the Kirkwood gaps or the extent of the depletion. To better understand these details, we will explore the 3:1 resonance, extending our simulations to much longer times. We will see evidence of *chaos* [3], and associated rare events which can provide an explanation of the depletion on astronomical time scales.

II. BACKGROUND

A. Elliptical orbits

First, we review several classical results on the Kepler problem [4] that will be needed in running and analyzing our simulations. When moving only in the gravitational field of the Sun a small body at position $\boldsymbol{r}$ feels an acceleration of

$$\boldsymbol{a} = -\frac{GM}{r^2}\hat{\boldsymbol{r}},$$

where M is the mass of the Sun and G is the universal gravitational constant. Solution of this equation of motion shows that, when bound, these bodies follow elliptical orbits with the Sun at one focus of the ellipse. These orbits can be characterized by the length of their semi-major axis, a, their eccentricity e and their relative orientation within the orbital plane (we will assume throughout a common orbital plane for all bodies). The distance from the Sun, r, can be written in a parametric form as

$$r = \frac{a(1-e^2)}{1+e\cos\theta},$$

where θ is the angle to the major axis of the ellipse. Alternatively we can use the perihelion and aphelion distances, $r_p = (1-e)a$ and $r_a = (1+e)a$, which represent the distances of closest and further approach from the Sun. The time-dependence of θ is non-trivial and can be defined implicitly using the equations

$$t = \frac{T}{2\pi}(E - e\sin E), \qquad \tan(\theta/2) = \sqrt{(1+e)/(1-e)}\tan(E/2), \tag{1}$$

where $T = 2\pi\sqrt{a^3/(GM)}$ is the period of the orbit and at $t = 0$ the body is at its perihelion. Determining $\theta(t)$ requires solving the above equation for $E(t)$ then using it to determine $\theta(t)$ and thus $r(t)$.

There are a number of relationships between the orbital parameters and the properties of the orbiting bodies that will be useful going forward, and can be found in textbook treatments of the Kepler problem [2, 4]. For setting the initial condition of a body, it will be useful to recall the *vis-viva* equation

$$v^2 = GM\left(\frac{2}{r} - \frac{1}{a}\right), \tag{2}$$

where v is the velocity of the body and a is its semi-major axis. At the aphelion this yields $v_a = \sqrt{GM/a(1-e)/(1+e)}$. We will also need to be able to determine the orbital parameters from its position and velocity at some fixed time. These can be obtained from the energy per unit mass $\epsilon \equiv |\boldsymbol{v}|^2/2 - GM/|\boldsymbol{r}|$ and angular momentum per unit mass $\ell \equiv |\boldsymbol{r}\times\boldsymbol{v}|$ via

$$a = \frac{GM}{2|\epsilon|}, \qquad e = \sqrt{1 + \frac{2\epsilon\ell^2}{G^2M^2}},$$

when the orbit is closed (and thus $\epsilon < 0$).

B. Jupiter's Orbit

Our primary goal is to model the combined effect of the Sun and Jupiter on the asteroid belt. We will fix the Sun at the origin and will model Jupiter's orbit as being solely due to the Sun, using the known semi-major axis $a_J \approx 7.7857 \cdot 10^8$ km ≈ 5.2044 AU and known eccentricity $e_J \approx 0.0489$ (since this is small, the orbit is nearly circular) [2]. Accordingly it has a perihelion and aphelion of $r_{p,J} = 4.9501$ AU and $r_{a,J} = 5.4588$ AU.

While we could obtain the Jupiter's position as a function of time directly from Eq. (1), by solving the non-linear equation at each time, we will instead compute Jupiter's orbit numerically for a single period and use interpolation to obtain any value of interest. Explicitly, we consider an initial position of the form

$$\boldsymbol{r}_J(0) = r_{J,a}\hat{\boldsymbol{x}}.$$

At the aphelion the velocity is perpendicular to $\boldsymbol{r}_J$ so we know the direction is along $\hat{\boldsymbol{y}}$. Its magnitude is fixed by the relation given in Eq. (2)

$$|\boldsymbol{v}_J(0)| = \sqrt{\frac{GM}{a_J}\left(\frac{1-e_J}{1+e_J}\right)} \approx 2.621 \text{ AU/year}.$$

A simulation of this orbit (using a fourth-order Runge-Kutta method [5]) is shown in Fig. 2.

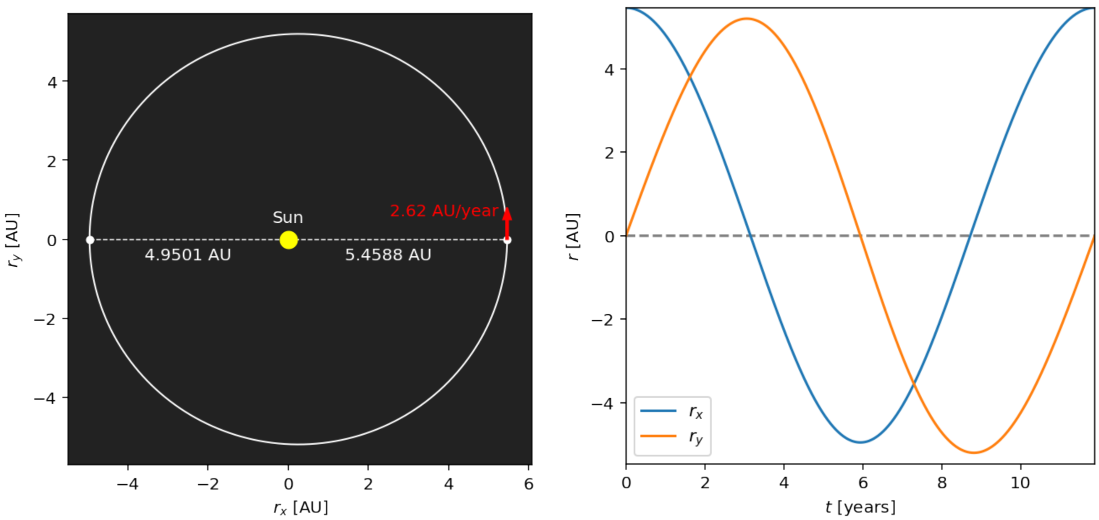

FIG. 2. (Left) Illustration of Jupiter's orbit and orbital parameters. (Right) Plot of the position of Jupiter over its period $T_J \approx 11.87$ years.

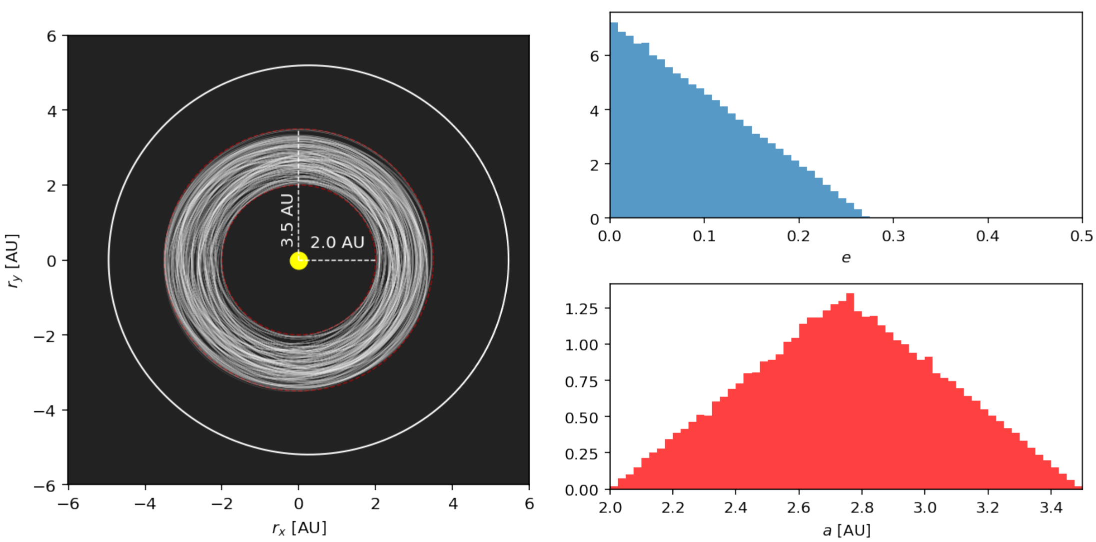

FIG. 3. (Left) Illustration of an ensemble of orbits with perihelion and aphelion with the bounds of the asteroid belt (range 2 AU to 3.5 AU). Jupiter's orbit is also shown. (Right) Orbital parameters (eccentricity and semi-major axis) for our randomly generated asteroids.

C. Asteroid belt orbits

We now need to look at the asteroid belt itself. What kind of initial conditions should we consider? For simplicity we will ignore the inclination of their orbits and assume they are all in the same plane as the planets. When discussing these orbits we'll also ignore the effects of Jupiter, and discuss the orbital properties arising from the Sun alone.

The bulk of the asteroids in the solar system lie in orbits with distances from the Sun in the range of 2 AU to 3.5 AU [2], well inside Jupiter's orbit. We will thus consider orbits such that the minimum and maximum distance (the perihelion and aphelion) lie in this range. We will generate a random asteroid trajectory by choosing r_a and r_p uniformly from this range (while keeping sure that $r_a > r_p$). The trajectory can be initialized following the same strategy we used for Jupiter, but allowing the angle of the semi-major axis (relative to Jupiter) to vary. In addition we need to consider the initial position of the asteroid along its orbit, given we set $t = 0$ such that Jupiter is at its aphelion. We thus specify a delay time t_0 for which we evolve the asteroid under the Sun's gravity alone to allow it to start at positions other than the aphelion.

Simulated trajectories of such an ensemble is shown in Fig. 3, along with a histogram of the initial distribution of the eccentricity and semi-major axis. We see that the distribution of eccentricities is peaked near $e = 0$ (circular orbits) with typical values of e in the range $0.1 - 0.25$. The semi-major axis distribution also has a bit of structure, being peaked in the middle of its range.

III. DYNAMICS IN THE ASTEROID BELT

We now turn to our primary problem of interest: an asteroid in the Sun-Jupiter system. The gravitational acceleration for a small asteroid with position $\boldsymbol{r}(t)$ under the influence of Jupiter and the Sun then takes the form

$$\frac{d^2\boldsymbol{r}(t)}{dt^2} = -GM\left[\frac{\boldsymbol{r}(t)}{|\boldsymbol{r}(t)|^3} + \alpha\left(\frac{\boldsymbol{r}(t) - \boldsymbol{r}_J(t)}{|\boldsymbol{r}(t) - \boldsymbol{r}_J(t)|^3}\right)\right]$$

where the position of Jupiter, $\boldsymbol{r}_J(t)$, is determined numerically as above and $\alpha \equiv M_J/M = 9.546 \cdot 10^{-4} M$ is the ratio of Jupiter's and the Sun's masses. Before embarking on simulations of this equation, we will try and understand *mean-motion resonances* that can appear when the period of $\boldsymbol{r}(t)$ is related to Jupiter's period by a rational number.

A. Mean-motion resonances

For generic positions of an asteroid of Jupiter the gravitational force is relatively small; Jupiter is light compared to the Sun and it is far away. Every so often they will pass close by each other, but if there is no relationship between their periods, this will likely be an irregular event, and we may expect that any influence it has on the asteroid's orbit might average to zero over time. However, if there *is* a relationship between their periods – so that

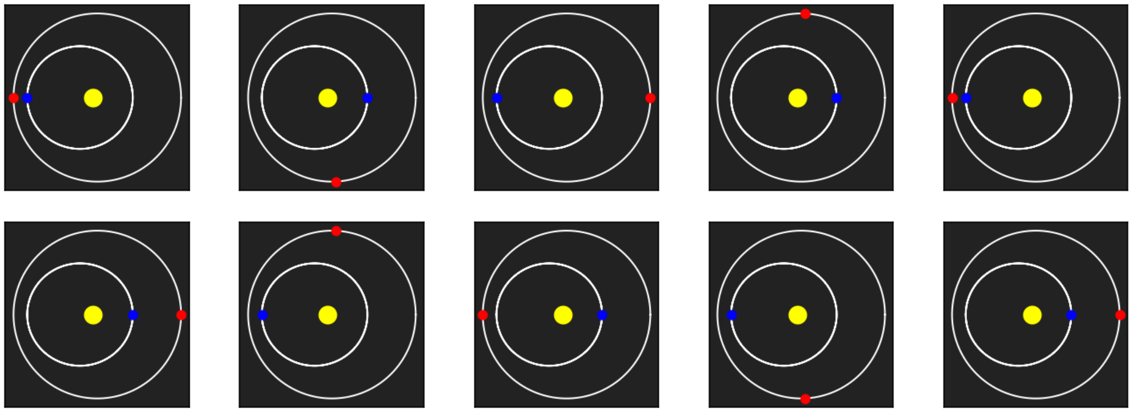

FIG. 4. (Top) Illustration of a 2:1 resonant orbit where the Jupiter (red) and the asteroid (blue) have close approaches every period T_J. Time is evolving from left to right in the figures and the asteroid orbit has eccentricity $e = 0.15$. (Bottom) Illustration of a 2:1 resonant orbit *without* close approaches.

they are in integer ratios – then any close encounters will repeat every common multiple of their periods. For example, if a *conjunction* occurs, i.e. where the bodies are at minimal possible distance where the gravitational force is maximal, then it will repeat over and over again due to their matching periods. The small effect of Jupiter's gravity will be amplified, accumulating over long times, and the asteroid's orbit can then be modified.

This can be illustrated simply for a 2:1 orbit, as shown in Fig. 4. In the top panels we see that Jupiter and the asteroid have a close approach during each of Jupiter's orbits. Over time this will lead a change in the semi-major axis and eccentricity of the asteroid. This is the essence of the phenomena of orbital resonance. We note that these resonant orbits are not *always* detrimental; in Fig. 4 we also have illustrated a stable configuration where their periods are in 2:1 resonance, but instead these close approaches are *avoided*.

More quantitatively consider Jupiter and the asteroid as being in circular orbits and they are in conjunction at time $t = 0$, following Ref.[2]. The next conjuction will then occur when

$$(\omega - \omega_J)\, t = 2\pi,$$

where $\omega = 2\pi/T$, $\omega_J \equiv 2\pi/T_J$ and T is the asteroid's period. Note the quantity $2\pi/T$ is also sometimes called the "mean-motion" of the orbit [2]. For an asteroid in resonance with ratio $n{:}m$ we define the period $T_J = (n/m)T_{n:m}$ and thus the semi-major axis (via Kepler's square-cube law)

$$a_{n:m} = \frac{a_J}{(n/m)^{2/3}},$$

where a_J is the semi-major axis of Jupiter. For example, for the 3:1 resonance, we have

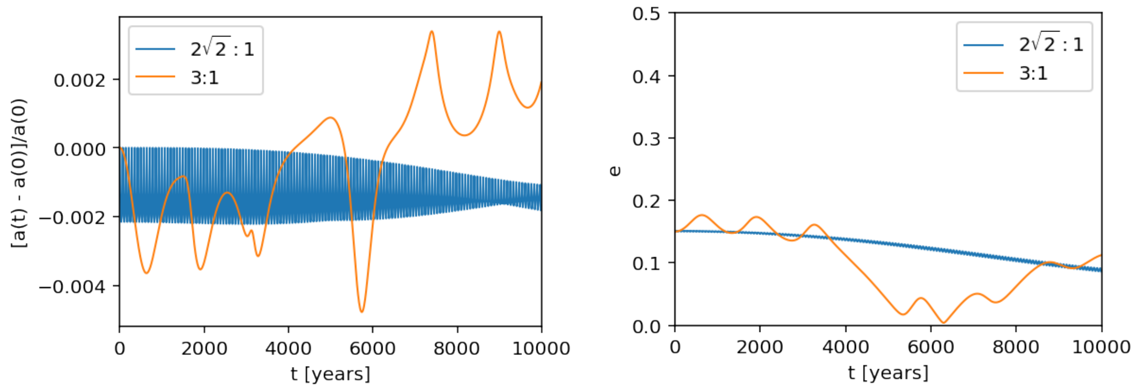

FIG. 5. Evolution of the semi-major axis (left) and eccentricity (right) of an initially elliptical orbit with eccentricity ($e = 0.15$), started at $t = 0$ at $0°$ relative to Jupiter for a resonant 3:1 period and for a non-resonant $2\sqrt{2}$:1 period. The time range is 10,000 years and we plot the result stroboscopically, showing one point for each of Jupiter's periods.

$a_{3:1} = a_J/3^{2/3} \approx 0.48075a_J \approx 2.502$ AU; about half of Jupiter's semi-major axis. The time of the next conjuction can then be written as

$$t = \frac{2\pi}{\omega_{n:m} - \omega_J} = T_J\left(\frac{n}{n-m}\right).$$

The average number of these conjunctions in a given stretch of time (much longer than T_J) thus $\propto 1/t$ and thus goes as $1 - m/n$. The *distance* of closest approach also varies with n:m; for circular orbits it is simply $a_J(1 - (m/n)^{2/3})$, and thus the gravitational effects scale as $(1 - (m/n)^{2/3})^{-2}$. We thus expect the average perturbation on the asteroid's orbit to go roughly as $(1 - m/n)/(1 - (m/n)^{2/3})^2$. For asteroids within Jupiter's orbit we have $n/m > 1$ and we see that this is monotonically increasing; we expect the strongest effects for small values of n/m, with correspondingly weaker effects as the ratio n/m increases. We note that this kind of analysis can also be carried out for elliptical orbits [2], though it is quite a bit more mathematically involved.

B. Resonant orbits

We will now explore the gaps themselves, focusing on orbits that are absent in the distribution of the asteroids. Our goal will be to see how the orbits become destabilized; in particular we want to know how long it takes for the effects of Jupiter to significantly affect the orbit of such an asteroid.

The first and most prominent resonance is when the asteroid's period is one-third that of Jupiter. To see the effect of Jupiter, we consider two initial orbits: one on the 3:1 resonance

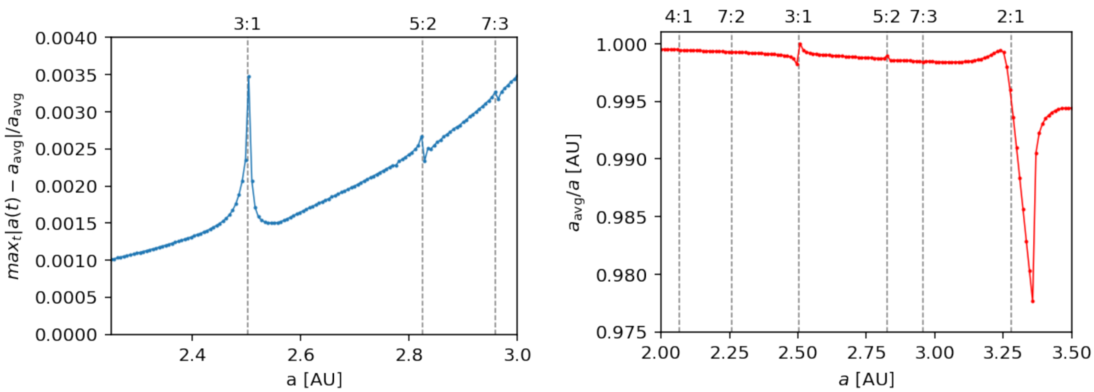

FIG. 6. (Left) The variation $\max_t |a(t) - a_{\rm avg}|/a_{\rm avg}$ of the semi-major axis of a circular orbit started a semi-major axis a. Evolution is for 1,000 years, and is zoomed on the structure of the semi-major axis whose near the 3:1, 5:2 and 7:3 resonances. (Right) Ratio of the average semi-major axis to the initial semi-major axis, $a_{\rm avg}/a$ for the same circular orbits, over the full range of the asteroid belt.

and one just off at $2\sqrt{2} : 1 \approx 2.82 : 1$. We will choose the eccentricity to be typical of our distribution, with $e = 0.15$ (see Fig. 3). We will track the effective orbital parameters of these objects over a long time period; several thousand years. The result is shown in Fig. 5. We see that the resonant orbit has much a much larger change in its semi-major axis than the non-resonant body. However neither are large in the absolute sense, with changes of less than 1% even over 1,000 years. The eccentricity changes more significantly for both the 3:1 vs $2\sqrt{2}$:1 orbits (more for the resonant than non-resonant orbit), but mostly stays below its initial $e = 0.15$ value.

To explore these effects more broadly we can consider an ensemble of orbits that start with a given semi-major axis and see how that semi-major axis changes as a function of time. For simplicity, we will use circular orbits and start the orbits in phase with Jupiter. We will aim to characterize the short-time (of order 1000 years) behaviour seen in Fig. 5. In Fig. 6 we quantify this in two ways: first using the range of variation of a as a function of time, and second as the shift in the average value of a over the time window. For both quantities we see that the resonances appear as strong peaks, with the 3:1, 5:2, 7:3 and 2:1 resonances being most visible (though the 2:1 resonance is broadened and shifted).

C. Kirkwood gaps

With some understanding of the effect of Jupiter's gravity, we now move to a more systematic exploration of the distribution of the asteroid belt. We will consider three sets of initial conditions:

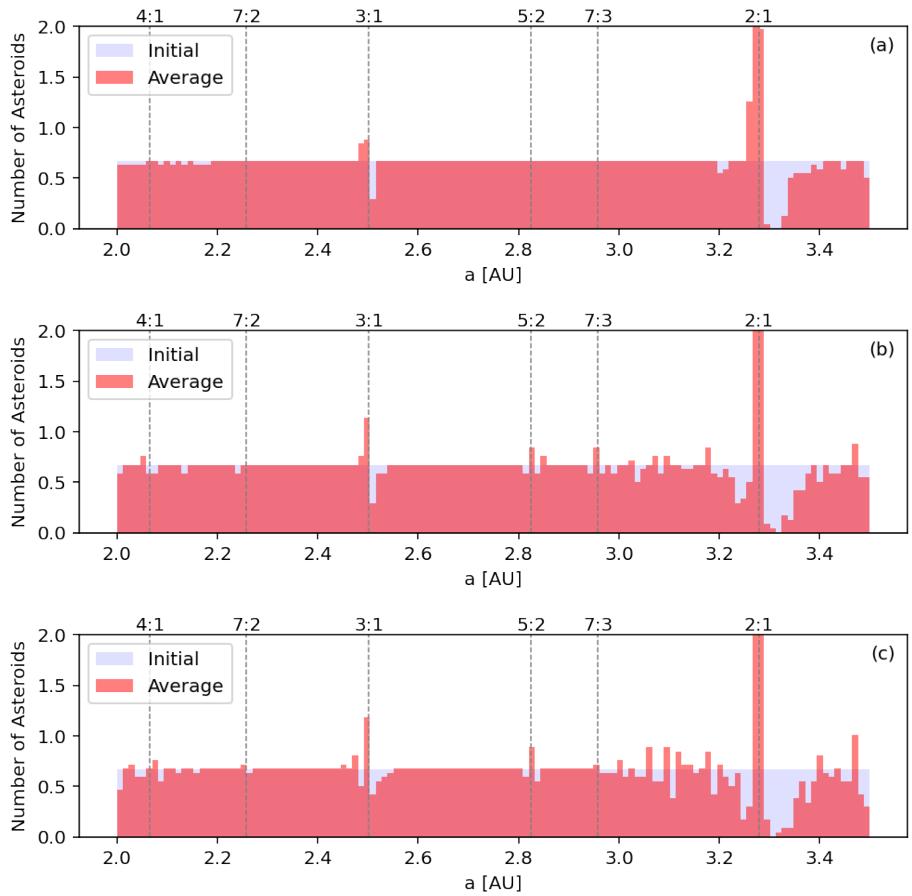

FIG. 7. (a-c) Histograms of the semi-major axis for (a) an ensemble of circular orbits with varying delay time, (b) an ensemble of elliptical orbits ($e = 0.15$) with varying orientation relative to Jupiter (delay time fixed) and (c) an ensemble of elliptical orbits ($e = 0.15$) with random orientation relative to Jupiter and random delay time.

(a). Circular orbits with 2 AU $\leq a \leq$ 3.5 AU. At each value of a we randomize the starting time $0 \leq t_0 \leq T$ of the circular orbit.

(b). Elliptical orbits with 2 AU $\leq a \leq$ 3.5 AU and fixed eccentricity $e = 0.15$. We set the delay time to zero (start at the aphelion) but randomize the orientation of the semi-major axis of the orbit, $0 \leq \theta \leq 2\pi$, relative to that of Jupiter.

(c). Elliptical orbits with 2 AU $\leq a \leq$ 3.5 AU and random eccentricity $0 \leq e \leq 0.25$, random delay time $0 \leq t_0 \leq T$ and random orientation $0 \leq \theta \leq 2\pi$.

The results are summarized in Fig. 7 where we show histograms of a binned over the full time range. We see that for each initial distribution of orbits (all are initially *flat* as

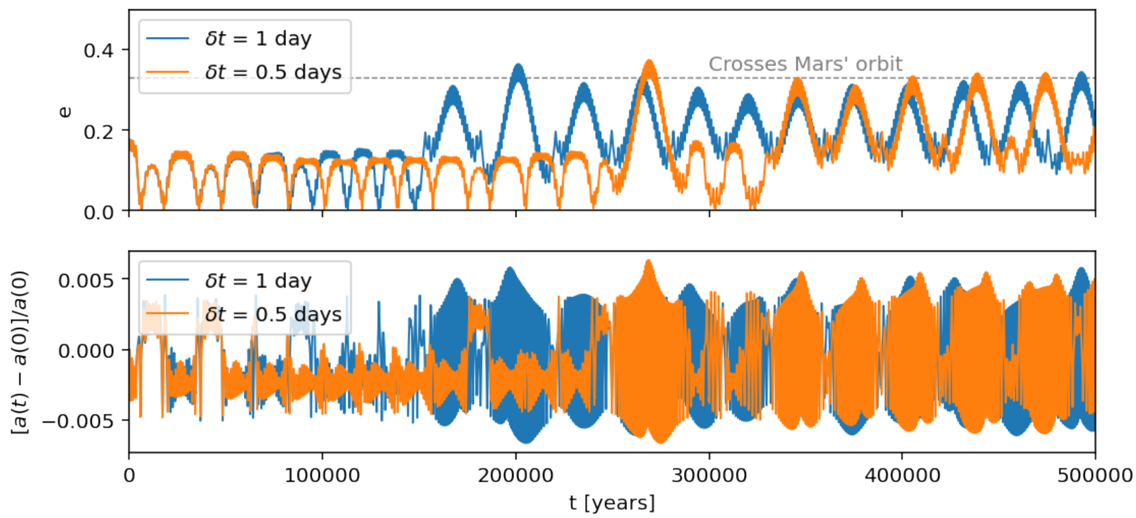

FIG. 8. Evolution of the eccentricity (top) and semi-major axis (bottom) of an initially elliptical orbit with eccentricity (e = 0.15), started at t = 0 at 0° relative to Jupiter for a resonant 3:1 period. The time range is 500, 000 years. Two different time steps are shown.

a function of a) there is evidence of removal of asteroid near the simple resonances. In particular the 2:1, 3:1 and 5:2 resonances are visible (to varying degrees in each).

D. Exploring the 3:1 resonance at long times

While we have reproduced some features of the Kirkwood gaps, we see from Fig. 1 and Fig. 7 that there are some qualitative differences. For example, the depletion of the 3:1 resonance is not as complete or as broad as seen in the solar system.

To understand what is going here, we focus on 3:1 resonant orbits, and consider simulations for much longer times than we managed in Sec. III B, to better approach astronomical time-scales (i.e. scales of order millions or billions of years). We revisit the same 3:1 orbit with e = 0.15, now extending the simulation to 500,000 years. As seen in Fig. 8, the behaviour of the semi-major axis is not too different over these time scales (still less than 1% change) though its oscillations become more erratic starting at 100,000 years.

However, looking at the eccentricity we see more dramatic behaviour: on the scale of one hundred thousand years we see that the eccentricity changes significantly, at points becoming as large as $e \approx 0.35$. These large changes in eccentricity are not just quantitative changes; when $e \gtrsim 0.33$ an orbit with a = 2.5 AU crosses the orbit of Mars. During one of these excursions to high eccentricity such an asteroid is likely to eventually pass close to Mars and have its orbit dramatically – either being ejected from the asteroid belt or being

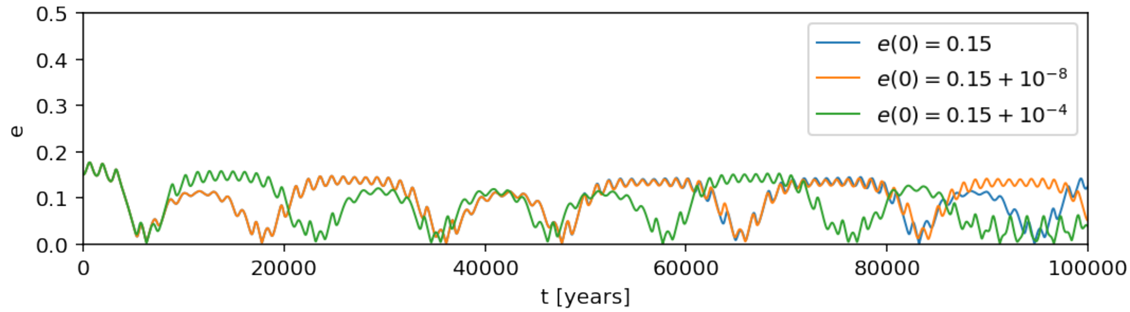

FIG. 9. Evolution of the eccentricity for a 3:1 resonant orbit with initial eccentricity, $e(0)$, near $e = 0.15$.

captured by Mars. Thus on the scale of millions of years we can expect the 3:1 resonance to be further depleted by these events.

These large changes are somewhat unpredictable; we see that over 100,000 years the eccentricity remains at or below its original value, behaving semi-regularly, until suddenly jumping. These sudden jumps are in fact related to chaotic behaviour [3, 6] in this system and depends crucially on the small eccentricity of Jupiter's orbit [3]. We can see some evidence for the chaos in the sensitivity of these trajectories at long times to the time steps used. Both time steps of 1 day and 0.5 days give physically plausible results, but diverge from each other over a time-scale of order 100,000 years or so. The presence of chaos can be inferred more directly by looking at small changes in the initial eccentricity. As shown in Fig. 9, even small changes of size 10^{-8} in the initial conditions quickly lead to qualitative differences in the orbit on time scales of order 100,000 years.

IV. METHODS

To simulate the orbits of Jupiter and of the asteroids we use the fourth-order Runge-Kutta method developed in class [5]. The symplectic methods are strictly speaking not applicable, given the external force being applied by Jupiter. They can still be useful given that over short times energy will approximately be conserved, but it is not clear that this will provide the needed stability at long times.

To determine the require time-step we examined our longest time and most sensitive calculation, the 3:1 resonant orbit evolved over a range of 10,000 years. Given we expect this orbit to eventually exhibit chaotic behaviour, we may anticipate some practical issues in matching different time-steps past some point in time. In Fig. 10 we show the evolution of $r_x(t)$ at 5,000 years and at 10,000 years of evolution using three different time steps: $\delta t = 1$ days, 5 days, 10 days. We see that the differences even at 5,000 years are minor and

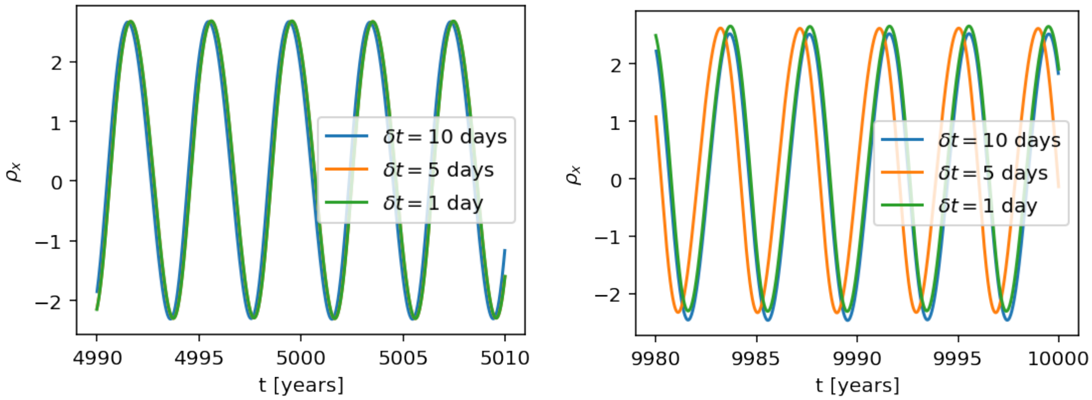

FIG. 10. Evolution of the $\hat{x}$ coordinate of a typical orbit ($e = 0.15$, $a = 2.5$ AU) over long times for three different time-steps.

thus a time-step of 10 days or less will be sufficient for the simulations we need. At 10,000 years we can see more significant differences, though some of this may be attributed to the chaotic nature of this system.

[1] Wikipedia, Kirkwood gap — Wikipedia (2021), [Online; accessed 15-March-2021] based on plot by Alan Chamberlain, JPL/Caltech.

[2] C. D. Murray and S. F. Dermott, *Solar system dynamics* (Cambridge University Press, 1999).

[3] J. Wisdom, Chaotic behavior and the origin of the 3:1 Kirkwood gap, Icarus **56**, 51 (1983).

[4] J. B. Marion and S. T. Thorton, *Classical Dynamics of Particles & Systems* (New York City, Harcourt Brace Jovanovich, 1986).

[5] M. Newman, *Computational physics* (CreateSpace Independent Publ., 2013).

[6] R. Malhotra, Orbital resonances and chaos in the solar system, in *Solar System Formation and Evolution*, Vol. 149 (1998) p. 37.